

First-Principles Study of Ti-Catalyzed Hydrogen Chemisorption on an Al Surface: A Critical First Step for Reversible Hydrogen Storage in NaAlH₄

Santanu Chaudhuri and James T Muckerman*

Department of Chemistry, Brookhaven National Laboratory, Upton, New York 11973-5000

Received: February 1, 2005; In Final Form: March 14, 2005

Complex metal hydrides are perhaps the most promising hydrogen storage materials for a gradual transformation to a hydrogen-based economy. We have used a computational approach to aid the ongoing experimental effort to understand the reversible hydrogen storage in Ti-doped NaAlH₄ and propose a plausible first step in the rehydrogenation mechanism. The study provides insight into the catalytic role played by the Ti atoms on an Al surface in the chemisorption of molecular hydrogen and identifies the local arrangement of the Ti atoms responsible for the process. Our results can potentially lead to ways of making other similar metal hydrides reversible.

I. Introduction

NaAlH₄ is a member of the family of complex metal hydrides, which are often represented as M_x(AH₄)_y (where, M = Li, Na, K, Rb, or Cs; A = Al, B, or Ga), that are of current interest for hydrogen storage. The recent surge in interest in them stems from their potential use in hydrogen fuel cells and all other possible mobile, lightweight hydrogen storage applications. NaAlH₄ is different from any other metal hydride and borohydride of similar structure because of its reported¹ reversible hydrogen storage capability when doped with Ti or Zr.

The reversible hydrogenation of NaAlH₄ occurs in two steps and can be summarized as follows^{2–5}



Remarkably, the hydrogen-depleted multicomponent products resulting from reaction 2 form large crystallites of the complex metal hydride upon the reverse reaction in the presence of titanium during hydrogenation, as has been observed by in situ diffraction studies. This is an important clue to understanding the role of Ti in that it implies a *concerted migration of metal atoms over large distances*. Local structural arrangements without the involvement of large-scale atomic migration would instead result in an amorphous or nanocrystalline structure. Under typical reaction conditions, i.e., temperature $T \approx 393 \text{ K}$ (120 °C) and 12 MPa H₂ pressure, it is unlikely that such large-scale mass transport occurs via bulk diffusion, but it probably proceeds via much faster surface and interfacial diffusion of specific mobile species. An intriguing observation concerns the dependence of the rehydrogenation kinetics on the amount of Ti doping. Typically, a level of 2 mol % Ti is required to initiate reversibility, while a saturation effect is observed at concentra-

tions of about 4 mol %. Recent experiments, suggesting that a large fraction of the Ti catalyst may reside in an under-coordinated environment, i.e., at or near the *surface* of the depleted material, could serve to rationalize this observation. Surface sites, exposed to hydrogen gas during rehydrogenation, are indeed the most likely sites for catalyzed H₂ dissociation and the subsequent formation of any hydrogen-containing mobile species. The combination of these factors suggests a focus on surface phenomena as the most promising strategy for identifying the effects of the Ti catalyst on reversible hydrogen storage in NaAlH₄.

None of the previous experimental studies^{2–5} provides an answer to the most critical question: *What is the role of Ti in the reverse reaction that forms NaAlH₄?* To address this question, we would like to incorporate into our model systems what we know about the oxidation state and coordination environment of Ti atoms in this multistep process as well as the location of the extremely dilute Ti species. The wealth of existing experimental data provides information on the structure of majority phases, energetics and kinetics of the chemisorption process, reaction rates,³ and microstructural changes. Some recent work^{6,7} also makes important observations regarding the Ti oxidation state and local coordination environment using in situ extended X-ray absorption fine structure (EXAFS) spectroscopy.

Our preliminary calculations showed that neither Al nor NaH surfaces dissociatively chemisorb molecular hydrogen. We have approached the problem of building model systems with these goals in mind: (a) find probable positions for the Ti atoms and the resultant structure of such a Ti-containing surface or nanocrystal, (b) identify the surface structure that is catalytically active, i.e., dissociates molecular hydrogen, and (c) study different means of transporting the hydrogen away from the active site to form stable aluminum hydrides. If we regard the H₂ and Al as having been expelled from the NaAlH₄ and Na₃-AlH₆ lattices during the dehydrogenation process (leaving NaH), the rehydrogenation must transport both H₂ and Al (perhaps as AlH₃ or some other Al_xH_n species) back into the NaH lattice.

* Author to whom correspondence should be addressed. E-mail: muckerma@bnl.gov.

We have chosen Al(001) for our model Al surface for three reasons: (1) the chemisorption of hydrogen atoms is energetically most favorable⁸ on an Al(001) surface, (2) Ti forms segregated regions of stable surface alloys on Al(001),^{9,10} which should be more favorable compared to a subsurface alloy for promoting reaction, and experimental indications point to localized Ti–Al phases, and (3) hydrogen also binds strongly to {001} microfacets (similar to the environment modeled in this work) in Al(111) steps making {001} a ubiquitous face for hydrogen absorption. This seems the simplest and most favorable scenario for Ti-assisted hydrogen dissociation on an Al surface.

II. Theoretical Methods

This study used the density functional theory program CASTEP¹¹ for most of the calculations presented here. We have employed the generalized gradient approximation (GGA) with a plane-wave pseudopotential (PWP) basis and the RPBE¹² functional to account for the exchange-correlation effects. An ultrasoft pseudopotential is used for the core electrons. All of the geometry optimization calculations were performed with a 270 eV energy cutoff with convergence criteria set at 2×10^{-5} eV/atom. The results were then further optimized for a finer k-mesh and a 310 eV energy cutoff for verifying the minima. Mulliken charge and overlap population analyses were performed using the pseudoatomic wave functions. In all cases, we have employed a spin-restricted (spin-unpolarized) approach with no net charge on the unit cell. Band structures and densities of states (DOS) of the different surfaces were calculated. Linear synchronous transit/quadratic synchronous transit (LST/QST) transition state (TS) searches¹³ were performed to look for transition states for the diffusion of the hydrogen atom on the doped metal surface and the diffusion barriers between various possible diffusion directions. This method first performs an LST search on the diffusion path between adjacent sites followed by conjugate gradient minimizations and QST maximization. Periodic first-principles molecular dynamics simulations were performed to understand the temperature effect on hydrogen diffusion. The time step used for the simulations was 2×10^{-15} s, and results from 1 ps simulations are reported here. Each simulation step performs an extended Lagrangian classical molecular dynamics (MD) step based on the forces calculated from the PWP density functional theory (DFT) technique described above. A significant speedup is possible in this otherwise costly method by using a variant of the wave function and the density extrapolation scheme originally proposed by Arias et al.¹⁴ The electrons were kept on the Born–Oppenheimer surface by explicitly minimizing the electronic part after each MD step. We preferred to employ NVT ensemble dynamics with Nosé–Hoover-type thermostats over NPT dynamics in the current calculations because of the lack of reliability of the latter in cases involving solid phase/gas phase interfaces.

Electronic structure calculations were started with atom positions from published crystallographic refinement results, and the unit cell parameters were validated by optimizing the unit cell. We notice no more than 1–2% deviation in the calculated unit cell parameters for the systems studied. This is important for establishing confidence in the functional (RPBE) used in this study. This functional is well-known for accurate predictions of surface reactions and chemisorption energies in metals, alloys, and other similar systems. The relaxed unit cells were used to form supercells and doped with an appropriate concentration of Ti atoms. Then the lowest energy surfaces were cleaved in a way to expose the Ti atoms for further study of structural

rearrangement and reactivity. The surfaces were relaxed to attain energy-minimized stable structures and were subsequently used to study absorption and reactivity of molecular hydrogen. The results presented here are based on periodic systems, i.e., a study of the Al(001) 2×2 surface is essentially an infinitely periodic surface composed of these 2×2 repeating units. The exposed surfaces in all of the cases were given a layer of vacuum as large as 25–30 Å to avoid interactions with its periodic image in the vertical direction. Our experience suggests that the above-mentioned separation and relaxation of two surface layers of atoms followed by a few fixed layers of Al atoms are the minimum requirement for achieving consistent energies and other ground-state properties. In this particular case, increasing the number of fixed Al layers does not have any significant effect apart from increasing the computational cost. All of our current calculations include 24 atoms in the periodic unit cell representing the surface, with two additional H atoms in the vacuum above the surface for studying dissociative chemisorption. Different orientations of an approaching hydrogen molecule have been considered.

Density functional theory as implemented in the DMol³ program^{15,16} was used to look at the orbitals involved in the multicenter bonding. This allowed us to replace the core treatment of CASTEP and a plane-wave basis set with atomic basis sets. Our calculation included 454 orbitals and 332 total electrons. We used a particular variation of numerical atomic basis sets called DNP (double numerical plus polarization). It includes a polarization p-function on all hydrogen atoms along with the d-functions used in DND basis sets. We used the same exchange-correlation functional (RPBE) in all calculations. Only the results showing orbital interactions between the surface highest occupied molecular orbital (HOMO) and hydrogen molecules are calculated by this all-electron method.

III. Results and Discussion

The current work uses density functional theory (DFT) to address the rehydrogenation process. We have studied four possible catalytic centers substituted into the surface of the depleted material, (1) Al(001) with one Ti atom, (2) Al(001) with two nearest-neighbor Ti atoms, (3) Al(001) with two next-nearest-neighbor Ti atoms as shown in Figure 1, and (4) NaH with a single Na replaced by Ti. Al metal itself has a very low affinity for hydrogen,^{17–19} but Ti doping changes the characteristics of the surface significantly. Our calculations of reactivity with molecular hydrogen on Ti-doped aluminum surfaces show that *only* the Al(001) surface containing two next-nearest-neighbor Ti atoms dissociates molecular hydrogen (Figure 2a shows the Al(001) surface before and after dissociation). The surface with a single Ti atom exhibits physisorption of H₂ with a Ti–H distance of approximately 2.1 Å. The surface with two nearest-neighbor Ti atoms has no observed affinity toward H₂. These results provide a strong indication that the particular local environment arising from two titanium atoms substituting for next-nearest-neighbor surface Al atoms is critical for the reaction.

On substitution of alternate Al atoms on the Al(001) surface by Ti, the initial linear chain of Al–Ti–Al–Ti becomes a zigzag Al–Ti–Al–Ti chain after surface reconstruction. The relaxed local structure resulting from this substitution can be described as a rhombus (diamond shape) with Ti atoms at opposite vertexes on the long diagonal and Al atoms at opposite vertexes on the short diagonal. Each of the Ti atoms in the surface cell is also part of a linear alternating Al–Ti–Al–Ti chain running in the direction perpendicular to the line joining the two visible

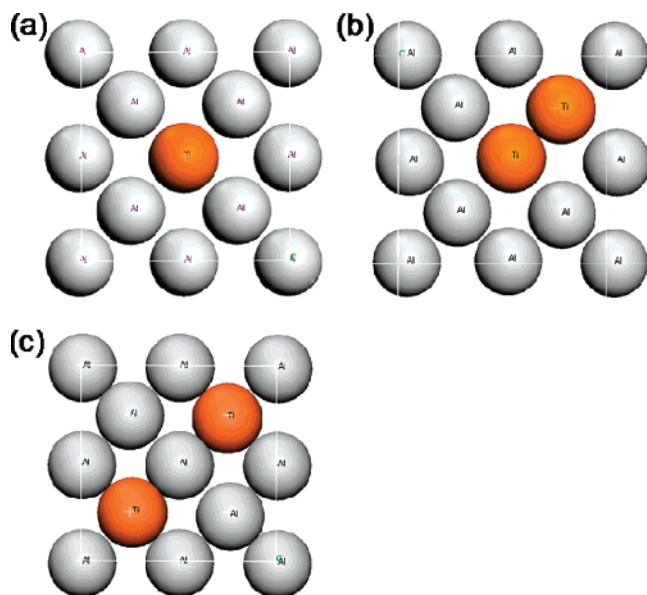


Figure 1. Arrangement of atoms on the top layer of the periodic unit cell before surface reconstruction formed by substituting Al atoms with (a) one Ti atom, (b) two nearest-neighbor, and (c) two next-nearest-neighbor Ti atoms, respectively, on a 2×2 Al(001) surface cleaved from the face-centered cubic lattice.

Ti atoms. (This can be visualized in Figure 3, which displays the close-packed surface layer resulting from periodic images of the surface considered here).

In the chemisorbed structure, the H atoms are nearly centered over triangular hollow sites consisting of one Ti atom and two Al atoms of the diamond-shaped surface structure (Figure 2b). The H–H distance after the dissociation is 2.04 Å. This process can also be described as the breaking of the H–H bond and the forming of partial Ti–H and Al–H bonds. Further, a Mulliken population analysis shows that the Ti atoms have a partial charge of +0.52, an increase from +0.29 calculated in the unreacted surface. These results are consistent with the Ti atom being less electronegative than both Al and H, such that Ti can donate more electron density to hydride formation than Al. It is also important that Ti does not form too strong of a bond with H in order for H migration to occur and free the active site. The chemisorbed structure (Figure 2b) has interesting bond overlap populations. The bond population analysis shows that the Al–H bonds are more populated, with overlap populations $n(\text{Al–H}) = 0.33$ and 0.32 , than the Ti–H bonds, with $n(\text{Ti–H}) = 0.14$. Thus formation of the chemisorbed structure is driven by Ti, but in the resultant structure the hydrogen atoms have significant bonding interactions with Al atoms. Such a situation is likely to be extremely important as the first step toward aluminum hydride (or alane) production and thus for the propagation of the reverse reaction and freeing up the catalytic centers (see discussion on the molecular dynamics of chemisorbed species below). The reaction is exothermic, and the chemisorption energy calculated with respect to the unreacted surface is -0.59 eV (-13.61 kcal/mol of H_2).

Some further all-electron DFT calculations with atomic orbital basis sets reveal an orbital picture that indicates why the alternate Ti–Al–Ti type of environment on a Ti-doped Al(001) surface is effective for dissociating a hydrogen molecule. These calculations show that the HOMO of the periodic surface (Figure 4a) involves the antibonding molecular orbital of the incoming hydrogen molecule (another view of only the surface orbitals is provided in the Supporting Information, Figure S1). The HOMO near the Ti atoms has a significant contribution from

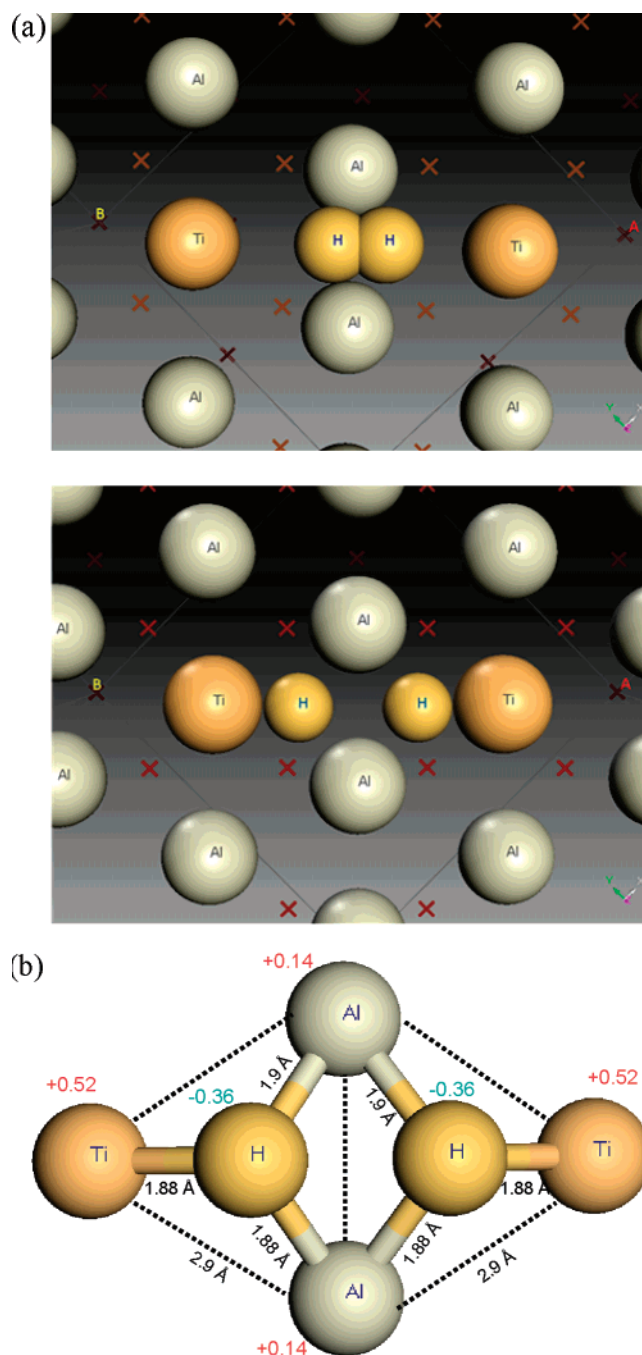


Figure 2. Relaxed Al(001) surface doped with two next-nearest-neighbor Ti atoms dissociates molecular hydrogen: (a) the surface before and after reaction and (b) structure and partial charges after dissociation showing hydrogen-occupied trigonal hollow sites. For clarity, the Al atoms from the layers below are shown as crosses.

the Ti 3d orbitals. The nodal symmetry of the surface HOMO is such that the incoming hydrogen σ^* can accommodate donated electron density from the Ti atoms. As a result, the σ bond of the molecular hydrogen is weakened and ultimately breaks. This indicates that the dissociation of hydrogen on such a surface is via the transfer of electron density from the surface to the incoming hydrogen molecule, consistent with metal hydride formation. The step-by-step dissociation of a hydrogen molecule is shown in Figure 4b. Such a reaction is not possible on an Al–Ti–Ti–Al-type surface structure because of a lack of suitable nodal symmetry of the HOMO of the surface– H_2 complex. The final chemisorbed structure (Figure 2b) has multicenter bonding involving the dissociated hydrogen atoms

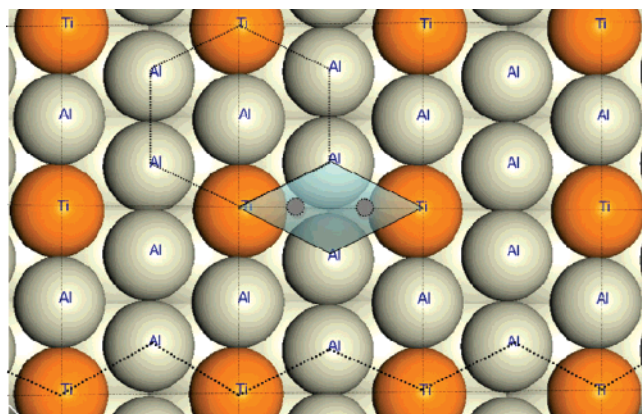


Figure 3. Extended periodic Al(001) surface layer doped with Ti showing both the rhombus, zigzag, and the alternating Ti–Al–Ti–Al chains. The gray circles are the hollow sites where the dissociated hydrogen atoms are located after chemisorption. The square lattice drawn on the surface is similar to (001) plane of the body-centered tetragonal TiAl_3 lattice in the arrangement of atoms although the distances in the bulk TiAl_3 are very different. The hexagonal unit shown is a building block for TiAl_3 hexagonal close-packed phase.

and the two Al atoms of the rhombus. The overall MO picture of this process (Supporting Information, Figure S2) involves crossing between the stabilized combination of the surface LUMO (incorporating two Ti $3d_{z^2}$ -like surface orbitals with opposite phases) and the σ^* of H_2 and the destabilized combination of the surface HOMO and the σ of H_2 , such that the pair of electrons that was originally in the surface HOMO ends up in the stabilized combination of the surface LUMO and the σ^* . The latter becomes the HOMO of the surface– H_2 adduct and is the orbital shown in Figure 4a and the Supporting Information, Figure S1. The net result is the population of the σ^* orbital, which leads to the cleavage of the H–H bond (Figure 4b). It is interesting to note that the hydrogen molecule donates σ electrons and at the same time accepts σ^* electrons from the doped metal surface. This is consistent with the accepted view of electron-transfer processes instrumental for hydrogen dissociation on metal surfaces.

The study of the fourth possible Ti environment, the NaH surface, also provides some interesting results that may or may not have implications for hydrogen storage. Our calculations show that Ti for Na replacement in a NaH(001) surface also leads to chemisorption of molecular hydrogen (Supporting Information, Figure S3) through the formation of a surface TiH_2 species (the exothermicity of the process is -0.94 eV or -21.86 kcal/mol of H_2). This result is supported by the reported²⁰ use of nanoscale NaH doped with Ti as a hydrogenation catalyst for terminal alkenes. It is, however, hard to imagine efficient ways of transporting this hydrogen to the Al lattice to form aluminum hydrides because it is strongly bound to the Ti atom and blocks the catalytically active site.

Hydrogen migration from a Ti–Al–Al hollow site to an Al–Al–Al hollow site is similar to what has been reported as alane formation on an Al metal surface. An LST/QST transition state (TS) search¹³ indicated the potential energy barrier between a Ti–Al–Al hollow site and an adjacent Al–Al–Al hollow site to be 1.57 eV for a perfect periodic surface and diffusion via an Al–H–Al bridging species. (The endothermicity of the process is 0.85 eV.) The presence of steps and defects in the Al metal surface could significantly lower this diffusion barrier. At lower temperatures, quantum tunneling will also have a significant contribution in the diffusion of hydrogen. Using a one-dimensional Eckart tunneling model and the calculated 91 li cm^{-1} tunneling frequency, we calculate a transmission factor

of 1.35 at 450 K and 8.16 at 100 K. We are not completely satisfied with the implementation of the LST/QST method in the CASTEP program and are currently carrying out a more rigorous reaction path search for lower-energy diffusion pathways.

We have carried out, using the same unit cell consisting of 26 atoms (including the dissociated hydrogen molecule) and starting from the minimum-energy chemisorbed structure, first-principles dynamics simulations at 350, 450, and 750 K to explore the probable transport route of the hydride species and of freeing up the catalytic site to drive the reverse reaction. The 0 K structure of dissociated H atoms occupying Ti–Al–Al hollow sites (Figure 2) on the surface changes significantly, with a hydrogen atom migrating to a neighboring hollow site (shown in the video in the Supporting Information) even at 350 K. The overall dynamic picture of the hydrogen atoms can be described as a back and forth motion between nearest-neighbor hollow sites. As a result of the high potential energy barrier (~ 1.57 eV) to enter an all-Al hollow site, even in molecular dynamics simulations at 750 K the hydrogen atoms move along the low-energy, high-mobility corridor over the Ti–H–Al bridges close to the Ti atoms.

The bond length distribution functions during a 1 ps simulation period were calculated for different atom pairs, Ti–Al, Al–H, and Ti–H. The calculated Ti–Al bond length distribution from the 350 K simulation data is a sum of two sharper distributions with maxima at 2.71 ± 0.02 Å and 2.80 ± 0.03 Å (the highest intensity peaks) and a broader subsidiary peak at longer Ti–Al distances around 3.0 ± 0.2 Å. The skewed nature of the distribution is due to a combination of the surface disorder and poor thermal averaging of lattice/surface vibrations on a short time scale (1000 steps with a 1 fs time step). The median of the Al–H distance distribution is at 1.84 ± 0.1 Å, which is longer than a normal Al–H bond (~ 1.6 Å) in NaAlH_4 or Na_3AlH_6 . The high mobility of the hydrogen atoms around the Ti atoms is reflected in larger widths of the Al–H and Ti–H distributions. The absence of hops to all-Al hollow sites in our MD results suggests that the most probable way for a hydrogen atom to diffuse away from the low-energy corridor is likely via quantum tunneling or conduits provided by local vacancies and other defects not included in the present model.

Recent experimental results point to processes very similar to what we propose here. We can identify two pivotal aspects of this rehydrogenation process where the experiments and our results need to be consistent: (1) the distribution of Ti atoms in the Al phase, i.e., the formation of TiAl_3 or a localized surface phase etc., and (2) the oxidation state of Ti before and after the reaction. Recent EXAFS data^{6,21} suggests the formation of a TiAl_3 alloy.²² We propose a slightly different model with emphasis on a particular Ti local coordination environment on the Al(001) surface. At a doping level of 2 mol %, the amount of titanium in a 20 nm diameter Al nanoparticle corresponds to 0.265 monolayers (ML). It is unlikely that a localized bulk phase of TiAl_3 would be formed under such a probabilistically unfavorable condition. Our suggestion of a particular local environment important for the chemisorption of hydrogen in the reverse reaction is further supported by the only major peak of the body-centered tetragonal TiAl_3 phase identified in the experimental diffraction results. The (001) Bragg plane in tetragonal TiAl_3 responsible for this major peak also locally contains both the alternating Al–Ti–Al–Ti chain and the Al–Ti rhombus arranged in perpendicular directions (Figure 3). Experimental results⁷ support our emphasis that there is no long-range order of this phase beyond one or two coordination

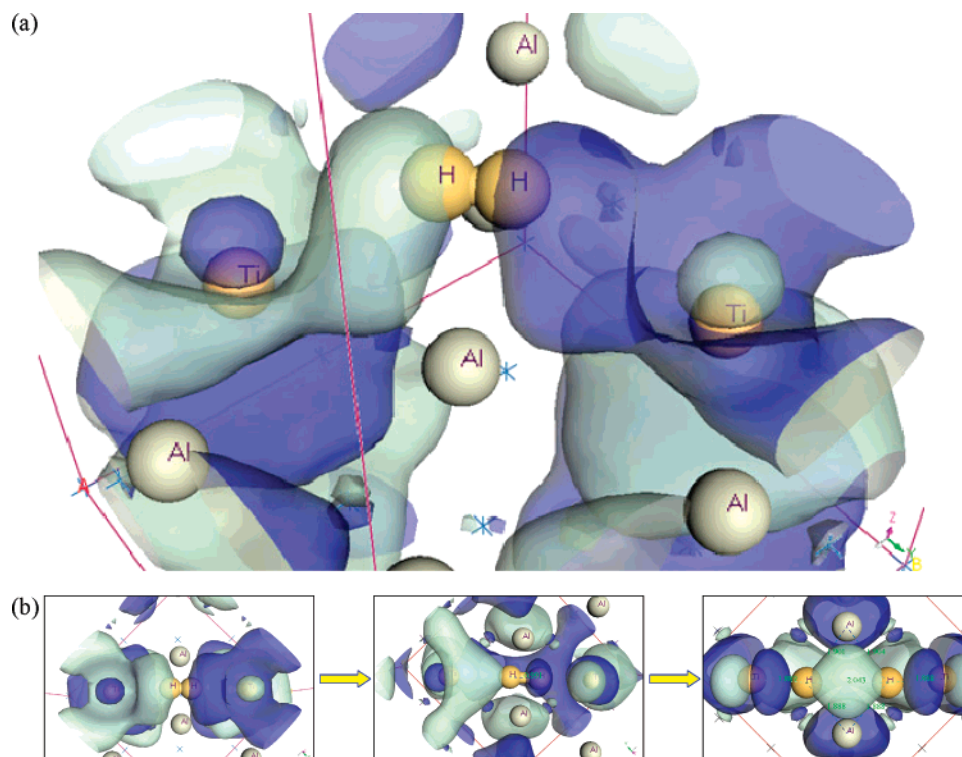


Figure 4. (a) The HOMO of the Ti-doped surface/ H_2 system showing the inclusion of the σ^* antibonding molecular orbital character of the incoming hydrogen molecule prior to the dissociation of the H–H bond. The dark and light blue shading indicates different signs of the orbital. In the vicinity of the two Ti atoms, the HOMO also shows considerable Ti 3d character. (b) Top view of the surface/HOMO during the dissociation of a hydrogen molecule showing electron density being transferred to the hydrogen σ^* orbital. The final structure after dissociation has two three-center bonds with atomic hydrogen.

spheres from a Ti atom, and the lowered average coordination number compared to a bulk phase suggests local and surface-dominated effects from small Al–Ti clusters. The average Ti–Al distance measured is approximately 2.8 Å, which is surprisingly similar to the one we obtain from first-principles MD results (2.80 ± 0.03 Å).

We also provide a detailed understanding of the oxidation state of Ti. Experimental studies have often proposed Ti^{3+} or Ti^{4+} as the catalytically active species without much further support than the comparison of overall catalytic activity based on initial dopant oxidation state. The EXAFS study⁶ of the depleted material supports our result of a Ti oxidation state between Ti^0 and Ti^{1+} . The formation of the chemisorbed hydrogen species in our calculations changes the Ti partial charge from +0.29 to +0.52. This is consistent with hydride formation on the surface and transfer of electron density from the vicinity of the Ti atoms to the hydrogen. The EXAFS data²¹ also shift toward a more oxidized Ti during hydrogenation. Finally, some transmission electron microscopy energy dispersive X-ray data²³ backed by EXAFS experiments note that the Ti ends up in the Al phase “entirely” and the local coordination environment around Ti atoms does not change over the dehydrogenation/rehydrogenation cycles. The only observed change is an increase in the concentration of Ti in the Al phase. This is also supportive of our view of the process wherein the Ti lowers the barrier for the formation of the Al_xH_n species but the core environment of the Ti–Al–Ti arrangement remains intact.

The above results can be summarized in three principal conclusions regarding the initial steps of reversible hydrogen storage in NaAlH_4 : (a) Ti atoms are indeed responsible for catalyzing the chemisorption of molecular hydrogen, (b) the presence of Ti is not enough, a particular local arrangement is

important for the rehydrogenation reaction, and (c) the diffusion of hydride species on the Al-metallic phase and the formation of alane species are probably the key to the synthesis of the next products in the rehydrogenation reaction. Once such detailed mechanistic information is known about the catalytic rehydrogenation of the depleted NaAlH_4 material, it can potentially lead to ways of making other similar metal hydrides reversible.

Acknowledgment. The authors thank Jon Hanson (Brookhaven National Laboratory (BNL)), Yan Gao (GE Global Research), and Jason Graetz (BNL) for insightful discussions regarding their concepts of the rehydrogenation reaction. This research is supported by the Catalysis and Chemical Transformations Program of the Division of Chemical Sciences, Geosciences, and Biosciences of the Office of Basic Energy Sciences of the Office of Science under Contract No. DE-AC02-98CH10886 with the U. S. Department of Energy. We also gratefully acknowledge support from the BNL Center for Functional Nanomaterials.

Supporting Information Available: Structure and origin of the Ti-doped Al(001) surface– H_2 HOMO, structure of the chemisorbed H_2 species on the Ti-doped NaH surface, and video of a 0.6 ps MD run at 350 K of the Ti-doped Al(001) surface– H_2 system. This material is available free of charge via the Internet at <http://pubs.acs.org>.

References and Notes

- (1) Bogdanovic, B.; Schwickardi, M. *J. Alloys Compd.* **1997**, 253, 1.
- (2) Bogdanovic, B.; Felderhoff, M.; Kaskel, S.; Pommerin, A.; Schlöcher, K.; Schuth, F. *Adv. Mater.* **2003**, 15, 1012.
- (3) Anton, D. L. *J. Alloys Compd.* **2003**, 356, 400.

- (4) Gross, K. J.; Sandrock, G.; Thomas, G. J. *J. Alloys Compd.* **2002**, 330, 691.
- (5) Jensen, C. M.; Gross, K. J. *Appl. Phys. A: Mater. Sci. Process.* **2001**, 72, 213.
- (6) Rijssenbeek, J. T.; Y. Gao; S. S. Srinivasan; Jensen, C. M.; J. Hanson; Wang, X. Characterization of Ti catalyst in NaAlH₄ doped with TiF₃. In *Proceedings of the Annual APS March Meeting*, Montreal, Quebec, Canada, March 22–26, 2004; American Physical Society: College Park, MD, 2004.
- (7) Graetz, J.; Ignatov, A. Y.; Tyson, T. A.; Reilly, J. J.; Johnson, J. Characterization of the Local Titanium Environment in Doped Sodium Aluminum Hydride using X-ray Absorption Spectroscopy. In *Proceedings of the Materials Research Society Fall Meeting*, Boston, Nov 29–Dec 3, 2004; Materials Research Society: Warrendale, PA, 2004.
- (8) Stumpf, R. *Phys. Rev. Lett.* **1997**, 78, 4454.
- (9) Kim, Y. W.; White, G. A.; Shivaparan, N. R.; Teter, M. A.; Smith, R. J. *Surf. Rev. Lett.* **1999**, 6, 775.
- (10) Saleh, A. A.; Shutthanandan, V.; Shivaparan, N. R.; Smith, R. J.; Tran, T. T.; Chambers, S. A. *Phys. Rev. B* **1997**, 56, 9841.
- (11) Segall, M. D.; Lindan, P. J. D.; Probert, M. J.; Pickard, C. J.; Hasnip, P. J.; Clark, S. J.; Payne, M. C. *J. Phys.: Condens. Matter* **2002**, 14, 2717.
- (12) Hammer, B.; Hansen, L. B.; Norskov, J. K. *Phys. Rev. B* **1999**, 59, 7413.
- (13) Halgren, T. A.; Lipscomb, W. N. *Chem. Phys. Lett.* **1977**, 49, 225.
- (14) Arias, T. A.; Payne, M. C.; Joannopoulos, J. D. *Phys. Rev. Lett.* **1992**, 69, 1077.
- (15) Delley, B. *J. Chem. Phys.* **1990**, 92, 508.
- (16) Delley, B. *J. Chem. Phys.* **2000**, 113, 7756.
- (17) Hammer, B.; Jacobsen, K. W.; Norskov, J. K. *Phys. Rev. Lett.* **1992**, 69, 1971.
- (18) Zhukov, V.; Ferstl, A.; Winkler, A.; Rendulic, K. D. *Chem. Phys. Lett.* **1994**, 222, 481.
- (19) Hammer, B.; Scheffler, M.; Jacobsen, K. W.; Norskov, J. K. *Phys. Rev. Lett.* **1994**, 73, 1400.
- (20) Fan, Y. H.; Liao, S. J.; Xu, J.; Wang, F. D.; Qian, Y. L.; Huang, J. L. *J. Catal.* **2002**, 205, 294.
- (21) Graetz, J.; Reilly, J. J.; Johnson, J.; Ignatov, A. Y.; Tyson, T. A. *Appl. Phys. Lett.* **2004**, 85, 500.
- (22) Hong, T.; Watsoyang, T. J.; Freeman, A. J.; Oguchi, T.; Xu, J. H. *Phys. Rev. B* **1990**, 41, 12462.
- (23) Felderhoff, M.; Klementiev, K.; Grunert, W.; Spliethoff, B.; Tesche, B.; von Colbe, J. M. B.; Bogdanovic, B.; Hartel, M.; Pommerin, A.; Schuth, F.; Weidenthaler, C. *Phys. Chem. Chem. Phys.* **2004**, 6, 4369.